

Electron transport and band structure of $\text{Ga}_{1-x}\text{Al}_x\text{As}$ alloys

H. J. Lee,* L. Y. Juravel,[†] and J. C. Woolley

Physics Department, University of Ottawa, Ottawa, Ontario K1N 6N5, Canada

A. J. SpringThorpe

Bell Northern Research Laboratories, Ottawa, Ontario, Canada

(Received 18 May 1979)

Measurements of electrical conductivity σ and Hall coefficient R_H have been made as a function of temperature in the range room to 230 °C on epitaxial n -type samples of $\text{Ga}_{1-x}\text{Al}_x\text{As}$ with carrier concentrations in the range 5×10^{21} to $1.6 \times 10^{24} \text{ m}^{-3}$. Theoretical calculations of σ and R_H have been made on a three-band (Γ , L , X) model using the method of Fletcher and Butcher, and the resulting values fitted to the experimental data by using the band-energy differences and various parameters in the electron-scattering equations as adjustable parameters. Thus the relative energy values of the three bands have been determined as a function of composition x , and values of such parameters as dielectric constant, deformation potentials, intervalley and interband coupling coefficients have been found. Different parameters dominate the results in different composition ranges, e.g., for $0 < x < 0.20$, the Γ and L bands have greatest effect, while for $0.7 < x < 1.0$ the X band is of major importance. However, the requirement that the various parameters vary smoothly with x has been used to extend the composition ranges for which the various parameters have been determined.

INTRODUCTION

$\text{Ga}_{1-x}\text{Al}_x\text{As}$ alloys have important optoelectronic applications, and hence various electrical and optical properties have been extensively investigated. Band-gap values have been determined from measurements of diode emission,¹ optical absorption,²⁻⁴ Schottky-barrier photoresponse,⁵ electroreflectance,⁶ and electron microprobe cathode luminescence.⁷ In most of this work, the energy E_0 of the Γ conduction-band minimum relative to the valence-band maximum ($\Gamma_1 - \Gamma_{15}$) has been the parameter of main interest with the $X_1 - \Gamma_{15}$ energy separation also being measured in the indirect-gap range and hence the composition at which the direct-indirect gap transition occurs being determined. However, the values of band gaps reported show considerable scatter differing by up to 150 meV. Little information is available about the $X_1 - \Gamma_{15}$ separation in the direct-gap range, and no data have been obtained on the $L_1 - \Gamma_{15}$ separation, although the electroreflectance measurements⁶ give values of the vertical transition energies at the L and X points. Various earlier experimental electron-transport data⁸⁻¹¹ were analyzed in terms of electrons in the Γ_1 and/or X_1 bands. However, the revised band structure of GaAs (Ref. 12) indicates that the L band can play an important part over a considerable composition range, particularly at temperatures above room temperature and, hence, analysis of electron-transport data must include the effects of electrons in the L band.¹³ At present, no values of scattering parameters are available for the L band.

Here, data for electrical conductivity and Hall coefficient as a function of temperature for values of x across the whole composition range have been fitted to calculated theoretical values, including Γ -, L -, and X -band contributions, the energy-band separations, and various scattering parameters being treated as adjustable.

EXPERIMENTAL MEASUREMENTS AND RESULTS

The $\text{Ga}_{1-x}\text{Al}_x\text{As}$ alloys used here were in the form of epitaxial layers grown on Cr-doped semi-insulating GaAs substrates.¹⁴ The uniformity of the layers has been carefully checked, and no variation in Al content has been observed in the direction of crystal growth, a $\langle 100 \rangle$ direction. The alloy compositions have been determined from photoluminescence and electron-probe microanalysis.

Twelve different alloy compositions have been investigated, doped with tellurium to produce suitable electron concentrations. The Hall coefficient R_H at 0.3T and the conductivity σ have been measured as a function of temperature from room to 230 °C using the van der Pauw method.¹⁵ The apparatus, accuracy of measurement, etc., were as described previously for similar measurements on GaAs.¹³ It was found that removal of the substrate from a specimen made no difference to the measured values, and, in the present temperature range, the room-temperature values obtained at the beginning of a temperature run agreed with those obtained when the sample was cooled down to room temperature again. Corrections for the effects of electrode

TABLE I. Room-temperature values for the twelve samples of $\text{Ga}_{1-x}\text{Al}_x\text{As}$ alloys. The Hall coefficients were measured at $0.3T$, and the values of N_A were obtained with the assumption that $N_{cc} = n_t + 2N_A$.

Sample No.	x	R_H ($10^{-5} \text{ m}^3 \text{ C}^{-1}$)	σ ($10^3 \Omega^{-1} \text{ m}^{-1}$)	n_t (10^{23} m^{-3})	N_A (10^{23} m^{-3})
1	0.08	126.2	0.329	0.052	0.22
2	0.11	0.405	51.50	15.84	2.30
3	0.13	0.525	39.60	12.23	1.90
4	0.23	0.512	29.89	13.20	4.13
5	0.27	0.729	17.20	8.80	5.10
6	0.30	2.025	5.26	3.90	7.15
7	0.34	2.55	4.32	3.57	6.20
8	0.40	7.39	1.09	1.41	
9	0.52	3.58	1.16	1.68	
10	0.60	2.30	1.85	2.58	
11	0.71	1.725	1.925	3.29	0.45
12	0.95	1.80	3.003	3.41	

size on the measured values have been made according to the analysis of Chwang *et al.*¹⁶

The room-temperature data for all compositions are given in Table I, and the curves of R_H and σ versus temperature for six samples of different composition are shown in Figs. 1-6. The variation with composition of the graphs of R_H and σ versus temperature is shown by this set of curves. With $x=0.106$ (Fig. 1), the curves are very similar to those for doped GaAs,¹³ indicating that all donors are fully ionized at room temperature and that the increase in R_H with temperature can be attributed to transfer of electrons to the L and X bands. For the case of $x=0.95$ (Fig. 6), the only band occupied is the X band, and the decrease in R_H with temperature is attributed to the activation of electrons from deep donor levels. The other figures show the transition from one con-

dition to the other, the increase in R_H due to deep donor effects being observed for the cases with $0.3 < x < 1.0$.

THEORY

In the multiconduction-band case, the zero-field conductivity and the Hall coefficient R_H may be expressed as¹⁷

$$\sigma = \sum_i n_i \mu_i e, \quad (1)$$

$$R_H = -\frac{1}{B} \frac{\sum_i D_i}{(\sum_i A_i)^2 + (\sum_i D_i)^2}, \quad (2)$$

where

$$A_i = n_i \mu_i e / (1 + r_i^2 F_i^2 \mu_i^2 B^2),$$

and

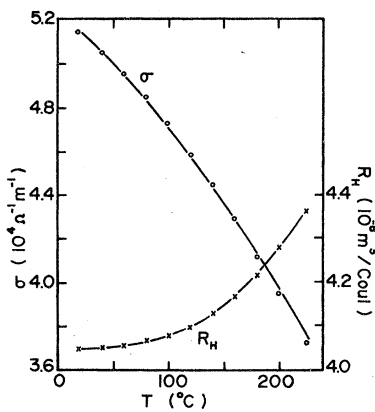


FIG. 1. Experimental values of Hall coefficient and conductivity as a function of temperature and theoretically fitted curve for sample No. 2 ($x=0.11$).

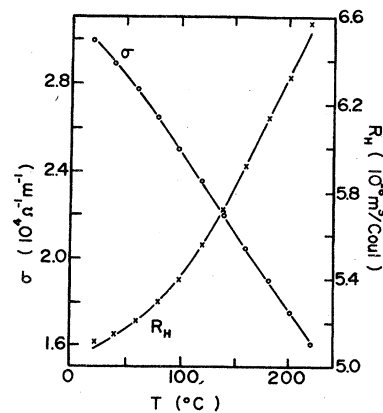


FIG. 2. Experimental values of Hall coefficient and conductivity as a function of temperature and theoretically fitted curves for sample No. 4 ($x=0.23$).

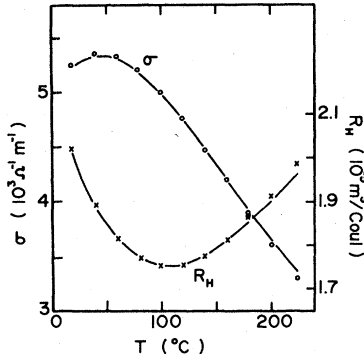


FIG. 3. Experimental values of Hall coefficient and conductivity as a function of temperature and theoretically fitted curves for sample No. 6 ($x=0.30$).

$$D_i = n_i \mu_i^2 e r_i F_i B / (1 + r_i^2 F_i^2 \mu_i^2 B^2)$$

i runs over all bands considered, with n_i the carrier density, μ_i the drift mobility, r_i the Hall scattering coefficient, F_i the anisotropy factor given by

$$F_i = \frac{2K_i(K_i + 2)}{(2K_i + 1)^2} \left(K_i = \frac{m_{ii}}{m_{it}} \right),$$

and B the magnetic field.

In the present analysis, it has been assumed that the Γ band has spherical constant-energy surfaces and has a nonparabolic form given by the Kane equation¹⁸

$$E = \frac{\hbar^2 k^2}{2m_e} + \frac{E_0^*}{2} \left\{ \left[1 + \frac{2\hbar^2 k^2}{m_e E_0^*} \left(\frac{m_e}{m_0} - 1 \right) \right]^{1/2} - 1 \right\}, \quad (3)$$

where E_0^* is the effective-mass band gap, m_0 the bottom-of-the-band effective mass, and m_e the free-electron mass. In the case of the L and X bands, a parabolic form has been assumed for

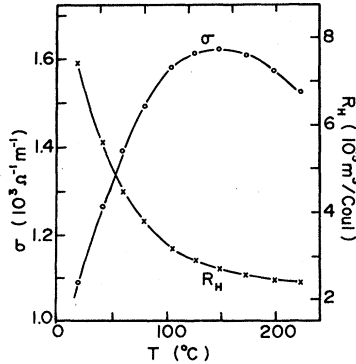


FIG. 4. Experimental values of Hall coefficient and conductivity as a function of temperature and theoretically fitted curves for sample No. 8 ($x=0.40$).

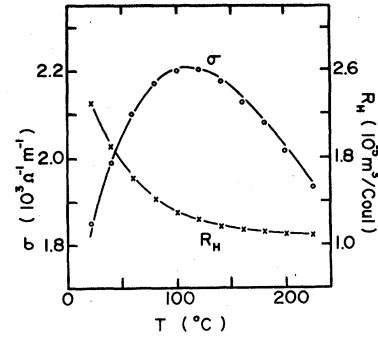


FIG. 5. Experimental values of Hall coefficient and conductivity as a function of temperature and theoretically fitted curves for sample No. 10 ($x=0.60$).

each, and, in consideration of transport and electron concentration, equations with spherical symmetry used with the density-of-states effective mass m_d written as $(m_l m_t^2)^{1/3}$ and the conductivity effective mass given by

$$\frac{1}{m_c} = \frac{1}{3} \left(\frac{1}{m_l} + \frac{2}{m_t} \right).$$

The temperature variation of the energy of each conduction-band minimum relative to the valence-band maximum has been assumed to be of the form¹⁹

$$E_i(T) = E_i(0) + \frac{\alpha_i T^2}{(\beta_i + T)}. \quad (4)$$

The variation with temperature of the bottom-of-the-band effective mass m_0 for the Γ minimum has been taken as¹⁸

$$\frac{m_t}{m_0} = 1 + \frac{P_1^2}{3} \left(\frac{2}{E_0^*} + \frac{1}{E_0^* + \Delta_0} \right), \quad (5)$$

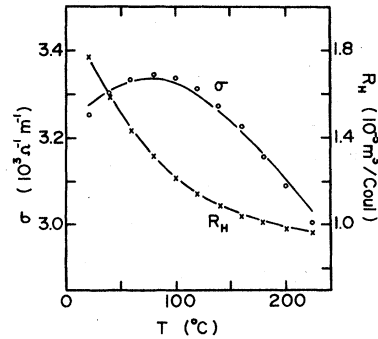


FIG. 6. Experimental values of Hall coefficient and conductivity as a function of temperature and theoretically fitted curves for sample No. 12 ($x=0.95$).

TABLE II. Parameter values for GaAs and AlAs assumed in the present analysis.

Parameter	GaAs	Ref.	AlAs	Ref.
$E_0(0)$	1.519 eV	32		
$m_0(0)$	$0.066m_e$	50, 51		
m_0 (room temp)	$0.0638m_e$	50		
γ_0	5.405×10^{-4} eV/K	32		
β_0	204 K	32		
Δ_0	0.34 eV	52	0.275 eV	33
E_1	3.04 eV	52		
Δ_1	0.22 eV	52	0.2 eV	33
m_{tL}	$0.0754m_e$	52	$0.15m_e$	41
m_{iL}	$1.9m_e$	12	$1.32m_e$	41
E_{02}	0.462 eV	12		
m_{tX}	$0.23m_e$	53	$0.19m_e$	55
m_{iX}	$1.3m_e$	54	$1.1m_e$	55
κ_∞	10.91	56		
κ_s	12.91	56	10.0	45
$\hbar\omega_0$	0.0362 eV	27	0.0474 eV	27
$\hbar\omega_{ij}$	$0.8\hbar\omega_0$	54	$0.8\hbar\omega_0$	54
C_i	1.397×10^{11} N/m ²	57	1.34×10^N /m ²	58
ρ	5307 kg/m ³	59	3598 kg/m ³	58

where the matrix element P_Γ^2 has been determined from the parameter values at absolute zero (see Table II), and the effective-mass band gap E_0^* taken as²⁰

$$E_0^* = E_0(0) - \frac{E_0(0) - E_0(T)}{a}, \quad (6)$$

where a is a constant independent of T . The values of E_0 and Δ_0 have been taken from electroreflectance data.⁶

The variation of m_{tL} for the L band has been taken as^{21,22}

$$\frac{m_e}{m_{tL}} = 1 + P_L^2 \left(\frac{1}{E_1} + \frac{1}{E_1 + \Delta_1} \right), \quad (7)$$

where E_1 is the vertical gap and Δ_1 the spin-orbit splitting at the L point, and the matrix element P_L^2 again is determined from the values at absolute zero. The room temperature values of E_1 and Δ_1 have been obtained from electroreflectance data,⁶ and the temperature dependence of E_1 assumed to be given by Eq. (3). The value of m_{iL} for the L band has been assumed temperature independent^{21,22} while, because the associated vertical band gap is large,⁶ the values of m_{iX} and m_{tX} for the X band have been assumed to be temperature independent also, the same assumption as was made for the case of GaAs.¹³

The carrier concentrations in the three bands have been taken as (in Ref. 20)

Γ band:

$$n_0 = 4\pi \left(\frac{2m_0 k_B T}{\hbar^2} \right)^{3/2} \left[F_{1/2}(\eta) + \left(\frac{5}{2} - 5\gamma \right) \beta F_{3/2}(\eta) + \left(\frac{7}{2} - \frac{21}{2}\gamma \right) \beta^2 F_{5/2}(\eta) - \left(\frac{1}{4} + \frac{7}{2}\gamma \right) \beta^3 F_{7/2}(\eta) \right], \quad (8)$$

where

$$\eta = \frac{E_F}{k_B T}, \quad \gamma = \frac{m_0}{m_e}, \quad \beta = \frac{k_B T}{E_0^*}$$

and

$$F_n(\eta) = \int_0^\infty \frac{x^n dx}{\exp(x - \eta) + 1}.$$

L and X bands:

$$n_i = 4\pi N_i \left(\frac{2m_{di} k_B T}{\hbar^2} \right)^{3/2} F_{1/2}(\eta - \xi_i), \quad (9)$$

where

$$\xi_i = \frac{E_i - E_0}{k_B T},$$

E_i is the energy of the minimum of the i th band relative to the top of the valence band, and N_i is the multiplicity of the i th band. The neutrality equation has been taken as

$$n_i = \sum_i n_i = N_{SD} + N_{DD} - N_{DN} - N_A, \quad (10)$$

where N_{SD} is the shallow donor concentration, N_{DD} the concentration of deep donors, N_A the concentration of compensated acceptors, and N_{DN} the concentration of un-ionized deep donors given by²²

$$N_{\text{DN}} = N_{\text{DD}} \{1 + g \exp[(-E_F - E_{\text{DD}})/k_B T]\}, \quad (11)$$

g being the degeneracy factor, and E_{DD} the activation energy of the ground state of the deep donors, the excited states of the donors being ignored.

The calculation of mobility values has been carried out as described previously for GaAs,¹³ using the Fletcher and Butcher (FB) method.²³ For the Γ band, the FB iterative solution of the Boltzmann equation has been used to calculate polar-optical-scattering effects, the effects of other scattering mechanisms being determined as relaxation time values and included in the iteration. For the L and X bands, a slightly easier, more approximate method has been employed by using the FB analysis to give an effective relaxation time for polar optical scattering and then including this in a standard relaxation-time approximation.²⁴

METHOD OF ANALYSIS

A large number of parameters are unknown and hence must be assumed or treated as adjustable in the analysis, and hence the question arises of whether a unique set of parameters satisfying all the results can be obtained. However, because of the differences in band structure across the alloy range, in certain ranges of composition and temperature only a small number of parameters is involved and these can be determined with good accuracy. As was the case for GaAs, for alloys in the range $0 < x < 0.15$ at the lower temperatures only the Γ band has effect with the L band coming in at higher temperatures and the X band having a small effect only at the highest temperatures investigated here. Thus, guided by the values for GaAs, Γ and L parameters can be determined in this composition range. At the other end of the alloy range, only the X band contributes when $0.6 < x < 1.0$, and hence here parameters appropriate to the X band are determined. Since all parameters can be expected to vary smoothly with x , extrapolation of the Γ and L parameters from the GaAs-rich values and interpolation of the X parameters from the AlAs-rich values to those of GaAs give a good guide to all parameter values in the central composition range where all three bands contribute. A continued iteration between the calculations at the various compositions thus has resulted in a set of parameters which give a consistent fit to the experimental data over the whole composition range.

In multiband transport calculations, the energy separations of the various bands are of major importance, and in the present work the energy values of the Γ , L , and X minima relative to the

valence-band maximum have been treated as adjustable parameters, the chosen values being guided by the known values for GaAs and AlAs and, for the Γ band, by the published results discussed above.¹⁻⁷ Monemar *et al.*⁴ showed that, for the Γ_1 and X_1 minima, the temperature coefficients of the minima are to a good approximation independent of x and hence here the temperature coefficients of the band gaps determined for GaAs (Ref. 13) have been assumed as starting points. With regard to the value of E_0^* , the a parameter in Eq. (4) has been assumed to have the value used for GaAs, i.e., $a = 1.6$.¹³ With these various energy-gap values, the temperature variations of the different effective masses are given by Eqs. (5)–(7). The mass values at absolute zero have been assumed to show a linear variation with x between the values for the two compounds, which are given in Table II.

In the calculation of mobility values, polar-optical scattering is very important in all three bands, and hence the dielectric constant κ_∞ is an important parameter in the calculations. No data are available on values of κ_∞ for these alloys, and the published experimental values for AlAs show considerable scatter (e.g., Refs. 25 and 26). Hence, here the value of κ_∞ has been assumed to vary linearly with x from the value determined for GaAs (Ref. 13), but the rate of variation with x and hence the value at AlAs has been treated as an adjustable parameter. For the static dielectric constant κ_s , it has been assumed that this varies linearly between the values for the two compounds (Table II).

For these alloys, Ilegems and Pearson²⁷ observed two longitudinal phonon branches of different energies, corresponding to those of the two compounds. For alloys near to a compound, the phonon intensity corresponding to the other compound is negligible. Thus for the three samples with $0 < x < 0.15$, the phonon energy for GaAs has been used here, while for $x = 0.95$ the value for AlAs has been used. Two-phonon effects are to be expected for other compositions but the present theory cannot deal with this. Hence in this composition range, a single-phonon energy has been assumed, linearly interpolated between the values for the compounds. Ehrenreich²⁸ used the same approximation for calculations on $\text{InAs}_{1-x}\text{P}_x$ alloys and concluded that it was reasonable. The phonon energy responsible for interband and intervalley scattering has been assumed to have the value of $0.8 \hbar\omega_0$ as in the case of GaAs.

Other required scattering parameters are the acoustic deformation potentials ($E_{D\Gamma}$, E_{DL} , and E_{DX}), the interband-scattering coupling coefficients ($D_{\Gamma L}$, $D_{\Gamma X}$, and D_{LX}), and the intervalley-scatter-

ing coupling coefficients (D_{LL} and D_{XX}). To simplify the analysis, it has been assumed that at any given x $E_{DL} = E_{DX} = E_{D\Gamma}$, $D_{\Gamma X} = D_{\Gamma L}$, and $D_{XX} = D_{LL}$, which appear reasonable assumptions in view of the results of the analysis of the GaAs data.¹³

The values of $E_{D\Gamma}$ (or E_{DX} depending on the range of x concerned), $D_{\Gamma L}$, and D_{LL} have been treated as adjustable with the initial assumption that each varies linearly with x . In the acoustic-scattering analysis, it has been assumed that the elastic constant C_1 also varies linearly with x .

One other scattering mechanism which needs to be considered here but did not apply for GaAs is alloy scattering.^{29,11} Because of uncertainty in the exact theoretical form for the relaxation time, here τ_{ai} has been written as

$$\frac{1}{\tau_{ai}(E)} = m_i^{3/2} x(x-1) E^{1/2} A_p, \quad (12)$$

where A_p is a constant independent of x , and m_i the effective mass of the electrons in the particular band considered. In the analysis it has been found that this scattering mechanism need be considered only for the X band in the indirect-gap range. Thus A_p has been treated as an adjustable parameter to be determined from fitting to samples with $0.5 < x < 1.0$.

The analysis of the data on the twelve samples investigated indicates that the eight samples with $0 < x < 0.4$ show direct-gap behavior while the other four have indirect gaps with the main contribution to the transport behavior from the X band. The details of the analysis can now be discussed for different ranges of x values, but, as indicated above, the analysis of each set of data had to be carried out many times with parameters continually adjusted in the light of values obtained at other x values, until a consistent fit to all the data was obtained.

For the three samples with $0 < x < 0.15$, the data are very similar to those for GaAs indicating that the effect of the X band is negligible except at the highest temperatures investigated. It has been found that the fit is more sensitive to small changes in the energies of the Γ and L minima than to small changes in the scattering parameters, and the experimental data have been initially fitted using the scattering parameters of GaAs and treating the energy values of the Γ and L minima and N_A , the compensated acceptor concentration, as adjustable. The best fit to the data gave values of E_0 , which are in good agreement with the earlier optical data^{5,6,31} and which are up to 50 meV lower than the recent values of Monemar *et al.*⁴ Slight adjustment of the scattering-parameter values to be consistent with those at higher values of x made very little dif-

ference to the values of E_0 obtained in the analysis. Thus in the fitting of data for samples with x greater than 0.15 values of E_0 , which were the mean of three previous publications,^{5,6,31} were used. A least-squares fit was made to these data plus the values obtained here for $0 < x < 0.15$, the values for GaAs (Ref. 32) and that for AlAs (Refs. 33) giving the relation for 22°C as

$$E_0 = 1.425 + 1.155x + 0.37x^2 \text{ eV}. \quad (13)$$

As indicated above, this is lower than the values of Monemar *et al.*,⁴ and the bowing parameter is considerably higher than the theoretically predicted values of 0.03 eV,³⁴ 0.05 eV,³⁵ and zero.³⁶ A similar discrepancy between experiment and theory has been obtained for $\text{Ga}_{1-x}\text{Al}_x\text{Sb}$ alloys.³⁷ Recent results by Casey³⁸ give E_0 (24°C) = 1.424 + 1.247 x in the direct-gap region, which at compositions close to the band crossover value ($x \sim 0.4$), would place the Γ_1 minimum about 20 meV below the value given by Eq. (13).

The behavior of the four samples with an indirect-band gap is dominated by the effects of the X band. Since in this case the conduction band is parabolic and the effective mass assumed independent of temperature, the energy of the X minima does not enter the analysis. Thus the transport values have in this case been fitted by adjusting the four parameters κ_∞ , D_{XX} , E_{DX} , and A_p . For the samples with $x = 0.71$ and $x = 0.95$, good fits have been obtained. However, in the case of samples with $x = 0.52$ and $x = 0.60$, the results of a one-band (X) calculation gave conductivity values a little smaller than the measured ones at the higher temperatures. Some contribution from the L band is to be expected in this range, and thus these higher temperature data have been fitted using a two-band (X and L) model adjusting only the energy of the L minima to give a fit, the values of all other parameters being estimated by extrapolation from the other x values.

In the case of the samples with $0.20 < x < 0.40$, all three conduction bands play important roles in determining the transport properties. In this composition range, the energy of the Γ minimum has been taken as given by Eq. 13, and the position of the L -band minima determined mainly by extrapolation from the values for the samples of lower x , only small adjustments being made to the assumed values. For the various scattering parameters, again the values were guided by the corresponding values at lower and higher x values. This left as adjustable parameters the energy of the X -band minima, guided by previously published values of the indirect-band gap^{2,5,39} and the value determined for GaAs,¹³

and also the scattering parameters $E_{D\Gamma}$, D_{LX} , $D_{\Gamma L}$, and D_{LL} . The values obtained for these various parameters are discussed below.

RESULTS AND DISCUSSION

The final curves fitted to the experimental data are shown in Figs. 1–6. For samples close to the two compounds, the data were fitted at all points to better than 1.5%. The worst fits, showing differences between calculated and experimental values of up to 3%, were for the samples with $x = 0.335$ and 0.52 . In both cases all three conduction bands contribute to the measured values, and the fitting problem is complicated. However, it is considered that, overall, the fit to the experimental data is good. From a consideration of the effects of changing the various parameters by small amounts from the final values, it is estimated that the errors in the energy values of the L and X minima will not exceed 20 meV at any composition. In the case of the scattering parameters, such as deformation potentials, interband and intervalley coupling coefficients, etc., when the relevant scattering mechanism is one of the dominant ones, the error in the scattering parameter will be relatively small and should not exceed 10%. However, if the scattering mechanism makes only a small contribution to the total scattering effect, the errors in the parameter can be up to 50%. The separate cases will be discussed below.

The final form for the variation of E_0 with x given by Eq. (13) has been discussed above. As was indicated there, it has been necessary to use the values given by Refs. 5, 6, and 31 to obtain a satisfactory fit to the experimental data. The energy values of the L_1 minima have been determined for ten samples in the range $0 < x < 0.60$, and a least-squares fit to the values obtained gives for 22 °C

$$E_L = 1.734 + 0.574x + 0.055x^2 \text{ eV}. \quad (14)$$

The bowing parameter in this case is considerably smaller than that for E_0 given in Eq. (13). The value of E_L for GaAs is 1.734 eV in good agreement with the value of 1.728 eV previously determined,¹³ while the value for AlAs is 2.363 eV. This is a little higher than the estimated value by Dingle *et al.* (quoted in Ref. 38) of 2.25–2.35 eV but lower than the theoretically calculated values of 2.57 eV (Ref. 40) and 2.76 eV.⁴¹

The energy of the X_1 minima has been determined for the samples with $0.20 < x < 0.40$, and a least-squares fit to these data plus the values for GaAs (Ref. 13) and AlAs (Ref. 42) gives for 22 °C

$$E_x = 1.911 + 0.005x + 0.245x^2 \text{ eV}. \quad (15)$$

This gives values in good agreement with the experimental data of Neumann and Junge³⁹ for the indirect-gap range, but in the range of band crossover ($0.4 < x < 0.5$) the values are about 20 meV lower than those of Dingle *et al.* (quoted in Ref. 38).

The final values of E_0 , E_L , and E_x used in the present analysis are shown in Fig. 7 together with the curves for Eqs. (13)–(15). With these values, the band crossover points at 22 °C can be shown to be

$$\Gamma - L: x = 0.432, E_0 = 1.992 \text{ eV}$$

$$\Gamma - X: x = 0.405, E_0 = 1.953 \text{ eV}$$

$$L - X: x = 0.350, E_L = 1.942 \text{ eV}.$$

Previous data indicated that the $\Gamma - X$ crossover occurred in the range from $x = 0.31$ (Ref. 36) to 0.5 .² Carey's estimate³⁸ from quoted data gives the $\Gamma - X$ crossover at $x = 0.45$ and the other two at values of x slightly higher than those obtained here.

With regard to the temperature variation of the band gaps, in the analysis the values of the α and β parameters for GaAs (Ref. 13) were used initially for all of the alloys in view of the results of Monemar *et al.*⁴ Since the values of E_0 had little effect on the fit over most of the range of x , no attempt was made to adjust the temperature dependence of E_0 . In the case of the L band, it was found that changes in the temperature coefficient of E_L spoiled the fit to the experimental data, and best results were obtained with the parameters corresponding to GaAs, i.e., $\alpha_L = (-7.80 \pm 0.10) \times 10^{-4}$ eV/K and $\beta_L = 490 \pm 5$ K. However, for the X band in the composition range $0.27 < x < 0.60$, it was found that the variation

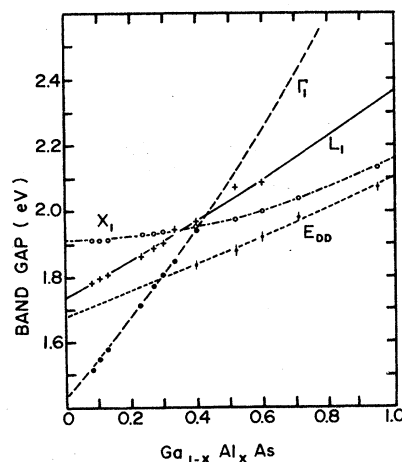


FIG. 7. Band-gap and deep donor energy as a function of x at 22 °C. The curves are given by Eqs. (13), (14), (15), and (20).

with temperature of the X_1 minima had to be smaller than that for GaAs to give the best fit. Thus the values of β_x was taken as that of GaAs, i.e., 550 ± 10 K, but α_x was taken as $-(6.2 \pm 0.2) \times 10^{-4}$ eV/K in this composition range.

The absolute-zero values of the effective mass for the Γ band were initially taken from Rode's estimate.⁴³ However, for good fits to the data, slightly higher values were needed and the final values obtained were

$$m_0(0)/m_e = 0.066 + 0.088x, \quad (16)$$

any bowing effect being neglected in view of the very small values of effective-mass bowing parameter for the various ternary alloys.⁴⁴ The above result gives a value of 0.154 ± 0.008 for AlAs in good agreement with the theoretical values of 0.15.^{40,41}

Turning to the analysis of the various scattering mechanisms, values for seven different parameters involved in the scattering process have been determined over different composition and temperature ranges. Values of the dielectric constant κ_∞ were determined in the composition range $0.5 < x < 1.0$, and these values together with that for GaAs were fitted to a linear variation in x giving

$$\kappa_\infty = 10.9 - 2.3x. \quad (17)$$

This result agrees with that of GaAs, of course, and gives a value of 8.6 ± 0.1 for AlAs which is in good agreement with the experimental value of 8.5 obtained by Monemar.⁴⁵ The values from Eq. (17) were used in the analysis of the data for all other samples.

The deformation potential for the Γ band ($E_{D\Gamma}$) was determined in the range $0 < x < 0.4$. Within the experimental scatter of ± 0.3 eV, in this composition range the results can be fitted to a linear variation of the form

$$E_{D\Gamma} = 16.1 - 13.5x \text{ eV} \quad (0 < x < 0.4). \quad (18)$$

However, in the composition range close to $x = 0.4$ there is some indication of curvature above this straight line, so that extrapolation of Eq. (18) beyond $x = 0.4$ may not be valid. As indicated above E_{DL} was assumed to have the same values as $E_{D\Gamma}$ as is the case for GaAs. However, E_{DX} was determined separately in the range $0.5 < x < 1.0$ and again, within that range, the values obtained could be fitted to the linear form

$$E_{DX} = 12.5 - 10.7x \text{ eV} \quad (0.5 < x < 1.0). \quad (19)$$

In this case, the extrapolated value at $x = 0$ is in good agreement with the value for GaAs of 12.5 ± 0.3 eV. The value for AlAs is thus given as 1.8 which appears very small but agreeing with

the value determined in the fitting to the data for the sample with $x = 0.95$. However, polar-optical scattering dominates in this range and the contribution of acoustic scattering is relatively small. Hence, as was indicated above, small errors in the fitted values of other parameters could lead to an appreciable systematic error in the values of E_{DX} given by the above equation.

With regard to the band-coupling coefficients, values of D_{XX} were determined in the range $0.5 < x < 1.0$ and fitted to the relation $D_{XX} = (5 - x)10^{10}$ eV/m. It has been assumed in the analysis that D_{LL} has the same values. Values of D_{LX} were determined in the range $0.20 < x < 0.40$, giving a linear fit of $D_{LX} = (11.0 - 10.5x)10^{10}$ eV/m in this range and agreeing with the value for GaAs.¹³ Only in the case of $D_{\Gamma L}$ could the values obtained not be fitted to a linear variation in the range investigated. In the range $0 < x < 0.25$ the values of $D_{\Gamma L}$ fell smoothly from that of $(8.0 \pm 1.0) \times 10^{10}$ eV/m for GaAs but leveled out in the range $0.3 < x < 0.4$ at a value of $(2.5 \pm 0.3) \times 10^{10}$ eV/m. This latter value is similar to that of 3×10^{10} eV/m quoted by Neumann and Flohrer⁴⁶ from Hall mobility calculations in the direct-indirect transition region. This type of variation with x may be due to the assumption that $D_{\Gamma L} = D_{\Gamma X} = D_{LX}$. Thus in the range $0 < x < 0.25$, effectively, the value of $D_{\Gamma L}$ is being determined while in the range $0.3 < x < 0.4$, D_{LX} plays the most important role.

Finally, for the case of alloy scattering the constant value A_p introduced in Eq. (12) was found to be $A_p = 4.6 \times 10^{68}$ mks. If Eq. (12) is compared with that given by Makowski and Glickman,²⁹ this value of A_p corresponds to an energy difference $|E_A - E_B| = 0.23$ eV. It has been suggested in earlier work that $|E_A - E_B|$ should be the difference between the energy gaps of the two compounds concerned, and clearly the present value is far lower than this. However, as indicated by Makowski and Glickman it is not at all clear how $|E_A - E_B|$ should be interpreted in a multiband problem. In the case of the sample with $x = 0.52$, the inclusion of alloy scattering reduced the calculated X -band mobility by approximately 12%, and the effect was smaller for other samples in this work. Maronchuk and Yakusheva¹¹ showed that the calculated mobility for the X band would be reduced by approximately 50% if $E_A - E_B$ were taken as the band-gap difference between the compounds, and such an effect would not allow any reasonable fit to the present data.

From the parameter values presented above, values of drift mobility can be calculated as a function of temperature for all the various scattering mechanisms and hence resultant values for

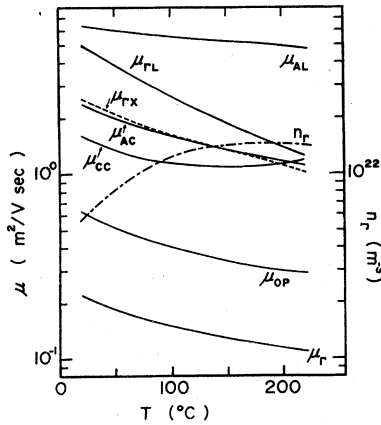


FIG. 8. Calculated variation of electron mobility and density with temperature in the Γ_1 band for sample No. 8 ($x=0.40$, $n_t=1.40 \times 10^{23} \text{ m}^{-3}$, and N_A negligible).

the three conduction bands. Such results are given in Figs. 8, 9, and 10 for the case of a sample with composition $x=0.40$ and total electron concentration at room temperature of $1.4 \times 10^{22} \text{ m}^{-3}$. Figure 8 shows the various mobility values for the Γ band and also the variation of n_Γ with temperature. It is seen that in this case polar-optical scattering is the dominant mechanism throughout the whole temperature range with only minor contributions from the other mechanisms. Of these, ionized impurity, acoustic deformation potential, and the two interband ($\Gamma-L$ and $\Gamma-X$) scatterings have similar mobility values at about 200°C while the effect of alloy scattering is considerably smaller. Although the value of $D_{\Gamma L}$ is much smaller than that for GaAs,¹³ interband scattering plays a more important role in the alloy because the bands are much closer

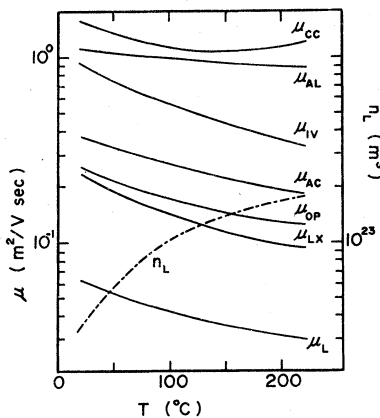


FIG. 9. Calculated variation of electron mobility and density with temperature in the L_1 band for sample No. 8 ($x=0.40$, $n_t=1.40 \times 10^{23} \text{ m}^{-3}$, and N_A negligible).

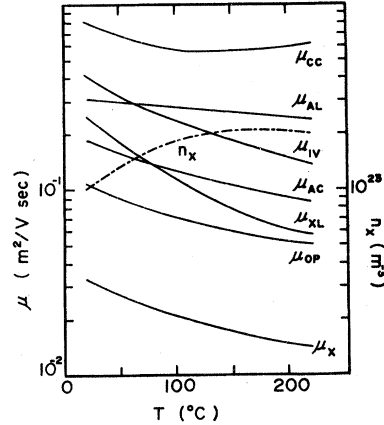


FIG. 10. Calculated variation of electron mobility and density with temperature in the X_1 band for sample No. 8 ($x=0.40$, $n_t=1.40 \times 10^{23} \text{ m}^{-3}$, and N_A negligible).

in energy in this case.

The values for the L band are shown in Fig. 9, where it is seen that the effect of interband ($L-X$) scattering is a little larger than that of polar optical with acoustic deformation potential having a smaller effect and the effects of the other scattering mechanisms being smaller still. For the X band (Fig. 10), again polar-optical scattering has the largest effect with interband ($X-L$) scattering making an appreciable contribution at the higher end of the temperature range. For GaAs, both $X-L$ interband and acoustic scattering had a larger effect than polar optical in the X band, this reflecting the results that the values of E_{DX} and D_{LX} , found for GaAs, were considerably larger than those determined for the alloy.

Values of room-temperature mobility for each band can be determined for each sample investigated, but comparison as a function of x is then difficult because of the different electron and compensated acceptor concentrations. Hence values of mobility at 20°C have been calculated for each band as a function of x for the case when the total carrier concentration $n_t=10^{22} \text{ m}^{-3}$ and $N_A=n_t$. The resulting curves are shown in Fig. 11 together with the calculated variation of the separate electron concentrations n_Γ , n_L , and n_X . It is seen that μ_Γ falls monotonically with x as is to be expected since polar-optical scattering dominates at all x values and the variation with x is due mainly to the corresponding increase in electron effective mass. In the range $0.3 < x < 0.5$, the relatively small effect of interband scattering can be observed. A similar result is observed for μ_X except that in this case there is an increase with x , again due to the variation of X -band effective mass. However, μ_L shows a minimum in

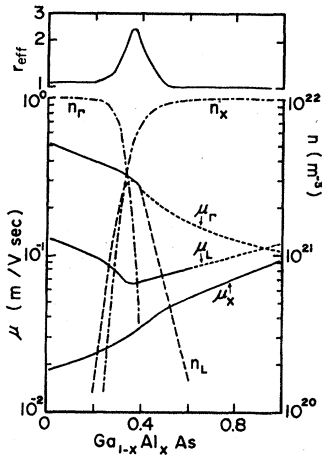


FIG. 11. Electron mobility, electron density, and effective Hall scattering coefficient at 22 °C as a function of x . Curves calculated for the case $n_t = 10^{22} \text{ m}^{-3}$ and $N_A = n_t$.

the range $0.35 < x < 0.40$ which can be attributed to the effects of interband scattering which, as can be seen from Fig. 9, is the most important scattering mechanism in this composition range. The effect of pressure on GaAs is to cause a similar variation in the relative energies of the conduction-band minima as that obtained in the alloys with variation of x , and curves showing the variation of the different mobilities with pressure have been calculated in this case (HJL and JCW, in press). As is to be expected, the GaAs curves are similar in form to those in Fig. 11 but a much more rapid variation in the range where all three bands are close in energy. The difference in the two sets of curves is due to the much lower values of the interband-scattering coefficient in the alloys compared with those for GaAs.

Also shown in Fig. 11 are the values of $r_{\text{eff}} = n_t R_H e$ for the case of $n_t = 10^{22} \text{ m}^{-3}$. This curve shows a maximum of $r_{\text{eff}} = 2.4$ at $x \sim 0.36$. Cor-

responding values for GaAs under pressure can be taken as the normalized Hall coefficient $R_H(P)/R_H(0)$, this quantity showing a maximum value in the range 2.5–4.5.⁴⁷

For samples in the range $0.3 < x < 1.0$, the analysis shows n_t increasing as a function of temperature, indicating the presence of deep donors. Values of E_{DD} and N_{DD} have been determined, the E_{DD} values being shown in Fig. 7. In this analysis, a single donor level associated with the X_1 minima has been assumed as in the case of Te-doped GaAs (Ref. 47) and thus the spin-degeneracy factor $g = 6$. The resulting values of $E_I (= E_X - E_{\text{DD}})$ are in the range 0.06 to 0.115 eV and the values of N_{DD} lie in the range 7×10^{23} to $1.6 \times 10^{24} \text{ m}^{-3}$. E_I is seen to fall with increasing x (Fig. 7), and similar E_I variation has been observed previously.^{8,14} By comparison with luminescence data, Neumann *et al.*⁸ suggested that the level is associated with silicon donors. The rate of decrease of E_I with increasing x is too large to be attributed to the effects of dielectric constant and effective-mass variations with x using a simple hydrogenic model. Also an E_I vs $N_{\text{DD}}^{1/3}$ relation^{30,47-49} does not appear to fit the present results. However, the impurity level may interact with more than one band, and thus the two-band (L and X) model of Aspnes¹² has been applied here, the effect of the Γ band being negligible because of its low effective mass. The value of E_I is then given by

$$E_I = \frac{1}{2}(E_X + E_L) - \frac{1}{2}[(E_X - E_L)^2 + 4V^2]^{1/2}, \quad (20)$$

where E_X and E_L are, respectively, the energies of the X and L minima relative to the valence-band maximum, and V is a constant independent of x . The present results have been fitted to Eq. (20), and a good fit obtained with $V = 0.12$ eV (see Fig. 7). This is to be compared with the value of $V = 0.18$ eV for the nitrogen level in the $\text{GaAs}_{1-x}\text{P}_x$ alloys.¹²

*Present address: Department of Physics, Jeonbuk National University, Jeonju, Seoul 520 Korea.

†Present address: Rockwell International, 3370 Miraloma Avenue, Anaheim, California 92803.

¹S. M. Ku and J. F. Black, *J. Appl. Phys.* **37**, 3733 (1966).

²J. F. Black and S. M. Ku, *J. Electrochem. Soc.* **113**, 249 (1966).

³M. B. Panish and S. Sumski, *J. Phys. Chem. Solids* **30**, 129 (1969).

⁴B. Monemar, K. K. Shik, and G. D. Pettit, *J. Appl. Phys.* **47**, 2604 (1976).

⁵H. C. Casey, Jr. and M. B. Panish, *J. Appl. Phys.* **40**, 4910 (1969).

⁶O. Berolo and J. C. Woolley, *Can. J. Phys.* **49**, 1335 (1971).

⁷A. Onton, M. R. Lorenz, and J. M. Woodall, *Bull. Am. Phys. Soc.* **16**, 371 (1971).

⁸H. Neumann, U. Flohrer, and W. Hörig, *Phys. Status Solidi A* **16**, 81 (1973).

⁹A. Yu. Matulenis, Yu. K. Pozhela, E. A. Shimulite, and V. Yu. Yutsene, *Fiz. Tekh. Poluprovodn.* **9**, 572 (1975) [*Sov. Phys. Semicond.* **9**, 379 (1975)].

¹⁰A. F. Kravchenko, Y. E. Maronchuk, and N. A. Yakusheva, *Phys. Status Solidi A* **30**, 543 (1975).

¹¹Y. E. Maronchuk and N. A. Yakusheva, *Fiz. Tekh. Poluprovodn.* **10**, 1349 (1976) [*Sov. Phys. Semicond.* **10**, 800 (1976)].

- ¹²D. E. Aspnes, *Phys. Rev. B* **14**, 5331 (1976).
- ¹³H. J. Lee, J. Basinski, L. Y. Juravel, and J. C. Woolley, *Can. J. Phys.* **57**, 233 (1979).
- ¹⁴A. J. Spring Thorpe, F. D. King, and A. Becke, *J. Electron. Mater.* **4**, 101 (1975).
- ¹⁵L. J. Van der Pauw, *Philips Res. Rep.* **13**, 1 (1958).
- ¹⁶R. Chwang, J. Smith, and C. R. Crowell, *Solid-State Electron.* **17**, 1217 (1974).
- ¹⁷R. A. Smith, *Semiconductors* (Cambridge University Press, New York, 1968).
- ¹⁸M. J. Aubin, M. B. Thomas, E. H. van Tongerloo, and J. C. Woolley, *Can. J. Phys.* **47**, 631 (1969).
- ¹⁹Y. P. Varshni, *Physica (Utrecht)* **34**, 149 (1967).
- ²⁰W. M. Coderre and J. C. Woolley, *Can. J. Phys.* **47**, 2553 (1969).
- ²¹M. Cardona and D. L. Greenaway, *Phys. Rev.* **125**, 1291 (1962).
- ²²J. S. Blakemore, *Semiconductor Statistics* (Pergamon, New York, 1962).
- ²³K. Fletcher and P. N. Butcher, *J. Phys. C* **5**, 212 (1972).
- ²⁴A. C. Beer, *Galvomagentic Effects in Semiconductors* (Academic, New York, 1963), Vol. 4.
- ²⁵R. E. Fern and A. Onton, *J. Appl. Phys.* **42**, 3499 (1971).
- ²⁶H. T. Minden, *Appl. Phys. Lett.* **17**, 358 (1971).
- ²⁷H. Hegems and G. L. Pearson, *Phys. Rev. B* **1**, 1576 (1970).
- ²⁸H. Ehrenreich, *J. Phys. Chem. Solids* **12**, 97 (1959).
- ²⁹L. Makowski and M. Glicksman, *J. Phys. Chem. Solids* **34**, 487 (1973).
- ³⁰H. C. Montgomery, *J. Appl. Phys.* **39**, 2002 (1968).
- ³¹M. B. Panish, *J. Appl. Phys.* **44**, 2667 (1973).
- ³²C. D. Thurmond, *J. Electrochem. Soc.* **122**, 1133 (1975).
- ³³A. Onton, in *Proceedings of the Tenth International Conference on the Physics of Semiconductors, U.S. AEC Division of Technical Information, Oak Ridge, Tennessee*, edited by S. P. Keller, J. C. Hensel, and F. Stern (Cambridge, New York, 1970), p. 107.
- ³⁴J. A. Van Vechten and K. T. Bergstresser, *Phys. Rev. B* **1**, 3351 (1970).
- ³⁵D. D. Sell, in *Proceedings of the Eleventh International Conference on the Physics of Semiconductors, Warsaw* (Polish Scientific Publishers, Warsaw, 1972), p. 1023.
- ³⁶A. Baldereschi, E. Hess, K. Maschke, H. Neumann, K. R. Schulze, and K. Unger, *J. Phys. C* **10**, 4709 (1977).
- ³⁷H. Mathieu, D. Auvergne, P. Merle, and K. C. Rustagi, *Phys. Rev. B* **12**, 5846 (1975).
- ³⁸H. C. Casey, Jr., *J. Appl. Phys.* **49**, 3684 (1978).
- ³⁹H. Neumann and W. Junge, *Phys. Status Solidi A* **34**, K39 (1976).
- ⁴⁰D. J. Stukel and R. N. Euwema, *Phys. Rev.* **188**, 1193 (1969).
- ⁴¹E. Hess, I. Topol, K. R. Schulze, H. Neumann, and K. Unger, *Phys. Status Solidi B* **55**, 187 (1973).
- ⁴²M. R. Lorenz, R. Chicotka, G. D. Pettit, and D. J. Dean, *Solid State Commun.* **8**, 693 (1970).
- ⁴³D. L. Rode, *J. Appl. Phys.* **45**, 3887 (1974).
- ⁴⁴O. Berolo, J. C. Woolley, and J. A. Van Vechten, *Phys. Rev. B* **8**, 3794 (1973).
- ⁴⁵B. Monemar, *Solid State Commun.* **8**, 2121 (1970).
- ⁴⁶H. Neumann and U. Flohrer, *Phys. Status Solidi A* **25**, K145 (1974).
- ⁴⁷G. D. Pitt and J. Lees, *Phys. Rev. B* **2**, 4144 (1970).
- ⁴⁸G. L. Pearson and J. Bardeen, *Phys. Rev.* **75**, 865 (1949).
- ⁴⁹H. P. Klug and H. Neumann, *Exp. Tech. Phys.* **XXIII**, 605 (1975).
- ⁵⁰R. A. Stradling and R. A. Wood, *J. Phys. C* **3**, L94 (1970).
- ⁵¹R. A. Stradling and R. A. Wood, *J. Phys. C* **4**, L38 (1971).
- ⁵²D. E. Aspnes and A. A. Studna, *Phys. Rev. B* **7**, 4605 (1973).
- ⁵³F. H. Pollak, C. W. Higginbotham, and M. Cardona, *J. Phys. Soc. Jpn. Suppl.* **21**, 20 (1966).
- ⁵⁴E. M. Conwell and M. O. Vassell, *Phys. Rev.* **166**, 797 (1968).
- ⁵⁵B. Rheinlander, H. Neumann, P. Fischer, and G. Kühn, *Phys. Status Solidi B* **49**, K167 (1972).
- ⁵⁶D. L. Rode, *Semiconductors and Semimetals*, edited by R. K. Willardson and A. C. Beer (Academic, New York, 1975), Vol. 10, p. 91.
- ⁵⁷D. L. Camphausen, G. A. N. Connel, and W. Paul, *Phys. Rev. Lett.* **26**, 184 (1971).
- ⁵⁸J. D. Wiley, *Semiconductors and Semimetals*, edited by R. K. Willardson and A. C. Beer (Academic, New York, 1975), Vol. 10, p. 221.
- ⁵⁹M. Neuberger, *Handbook of Electronic Materials III-V Semiconducting Compounds* (Plenum, New York, 1971), Vol. 2.